CrossMark

Determination of soil erosion risk using RUSLE model and soil organic carbon loss in Alaca catchment (Central Black Sea region, Turkey)

Ali Imamoglu[1] · Orhan Dengiz[2]

Abstract Soil erosion is one of the major threats to the conservation of soil and water resources. For that reason, predictive erosion models are useful tools for evaluating soil erosion and developing soil erosion management plans. For this aim, the revised universal soil loss equation (RUSLE) function is a widely used erosion model. This research integrated the RUSLE with a geographic information system (GIS) to investigate the spatial distribution of annual soil loss potential in the Alaca catchment in north central Black Sea region, Turkey. The rainfall erosivity factor was developed from local annual precipitation data using a modified Fournier index; the topographic factor was developed from a digital elevation model; the land cover factor was generated from satellite imagery and forest inventory maps; and the soil organic carbon level and the erodibility factor were developed from systematically collected soil samples and the application of the geostatistical method, respectively. From the model, more than the half of the total study area was in the very low and low erosion risk classes (0–12 t ha^{-1} year^{-1}), whereas 4.4 % (723.6 h) of the total area was at high and very high erosion risk (35–150 and >150 t ha^{-1} year^{-1}), respectively. In addition, soil organic carbon density values were between 0.18 and 4.92 kg m^{-2} across the catchment. Moreover, the distribution of soil organic carbon losses was closely correlated with the distribution of soil erosion risk classes in the study area. Soils and topographical properties of the watershed had a greater influence than land use/land-cover type on the magnitude of potential soil and soil organic carbon losses, because the erosivity factor did not change substantially in the study area.

Keywords RUSLE · Soil organic carbon · GIS · Alaca Basin

1 Introduction

Land degradation is causing serious social, economic, and environmental problems worldwide, especially in the more vulnerable areas with an arid or semiarid climate. Jones and Montanarella (2003) reported that land degradation is the reduction or loss in arid, semi-arid, and dry sub-humid areas of the biological or economic productivity and complexity of rain-fed cropland, irrigated cropland, rangeland, pastures, forests, and woodlands, including processes arising from human activities and habitation patterns. Therefore, land degradation directly affects livelihoods and food security, particularly in dry areas with unfavorable climate, by reducing the productivity of land resources and adversely affecting the stability, functions, and services derived from natural systems (UNCCD 2015). The types and causes of land degradation vary from one site to another, even within a short distance. Essentially, land degradation is the result of the misuse/overexploitation of the natural resources base, particularly through inappropriate and unsuitable agricultural practices, overgrazing, deforestation, and forest degradation (Dengiz et al. 2015). Moreover, in recent decades, the degradation of previously naturally vegetated or productive agricultural

✉ Orhan Dengiz
dengizorhan@gmail.com

Ali Imamoglu
aliimamoglu@yandex.com

1   Department of Geography Science, Faculty of Arts and Sciences, Ondokuz Mayis University, Samsun, Turkey

2   Department of Soil Science, Agricultural Faculty, Ondokuz Mayis University, Samsun, Turkey

lands, leading in many cases to a barren, desertified landscape, has dramatically accelerated in many regions of the world (Pla 2008).

The important functions of natural resources, especially soils, are threatened by many severe degradation processes. One of the major degrading factors is soil erosion caused by wind and/or water. RIVM (2000) stated that water erosion is one of the most important land degradation processes for EU countries. It was also reported that southern EU countries are at greater risk of water erosion, with high water erosion risk rates of 58, 66, 66, and 85 % in France, Italy, Spain, and Greece, respectively. Turkey is a hilly to mountainous country. The average elevation is approximately 1250 m, and 62.5 % of the total land has more than 15 % slope. Due to its topographic limitations (generally steep or sloping terrain) and to climate and soil conditions, soil erosion is Turkey's biggest land degradation problem; some 58.7 % of the land is exposed to severe or very severe soil erosion (Ministry of Agriculture, Forestry and Villages 1987). In addition, there is active erosion in 59 % of agricultural lands, 54 % of forest lands, and 64 % of rangelands of Turkey.

The soil organic carbon content is a key component of any terrestrial ecosystem, and any change in its abundance and composition has substantial effects on many of the processes in the system. Closely linked to the process of soil erosion is the widespread and substantial decline in soil organic carbon content in arid and semi-arid areas. Soil organic carbon, which is extremely important in all soil processes, is essentially derived from plant and animal residues, and is produced by microbes and decomposed at a rate determined by temperature, moisture, and ambient soil conditions. There are two groups of factors that influence soil organic carbon level; natural factors (climate, soil parent material, land cover and/or vegetation type, and topography) and human-induced factors (land use, management, and degradation).

Simulation models are the most effective means of predicting soil erosion processes and their effects through the use of geographic information system (GIS) and remote sensing (RS) for large areas. Recent advances in space and computer technologies have provided us with the opportunity to process large amounts of data (multi-source), not only spectral data but data such as elevation, slope, aspect and relief (Bayramin 1998). Therefore, models have the potential to make major contributions toward developing better conservation practices and improving the management of land resources (Meyer 1980; Edwards et al. 2008; Csafordi et al. 2012).

Empirical models, such as the universal soil loss equation (USLE) and its revised version RUSLE (Renard et al. 1991), have been used in many regions for large scale catchment risk mapping. Burrough (1986) introduced the

principles of GIS tools for collecting, storing, manipulating, and displaying spatial data, and Eedy (1995) reported the advantages of using GIS in environmental assessment. The estimation of soil erosion risk and its spatial distribution can be performed at reasonable cost and with improved accuracy across larger areas using RS and GIS techniques (Millward and Mersey 1999; Wang et al. 2003). Ouyang and Bartholic (2001) developed an interactive web-based approach to using RUSLE and GIS to predict soil erosion and Martin et al. (2003) used a GIS/RUSLE model to estimate sheet erosion in a watershed. They reported the ease with which GIS could be integrated with the RUSLE to identify discrete locations with relatively precise spatial boundaries that have a high sheet erosion potential together with the areas where management practices might be implemented to prevent soil erosion. Martin et al. (2003) also stated that GIS/RUSLE modeling represented a quick and inexpensive tool for estimating sheet erosion within watersheds when using publicly available information. Furthermore, Lu et al. (2004) applied RUSLE, remote sensing and GIS to the mapping of soil erosion risk in the Brazilian Amazonia. To contribute to improved land management practices and to establishing sustainable natural resources and environmental assessment in Turkey, the main objective of the current research was to integrate GIS and RUSLE to model soil erosion risk and carbon loss in a catchment in the Central Black Sea region.

2 Materials and methods

2.1 Field description of the study area

This study was carried out in the Alaca catchment which is located in Çorum and Yozgat Provinces in the Central Black Sea region of Turkey (Fig. 1).

The total study area is 1656.4 km². Geological formations in the catchment are generally dominated by Mesozoic–Tertiary ophiolitic series and limestones. In addition, the low lying lands of the study area are occupied by Quaternary alluvial and colluvial deposits, consisting of mixed gravel materials. The study area consists of various topographic features and is characterized by mountains (especially intermediate and low relief mountain ranges), hills and plains, and the south-western and south-eastern areas are characterized by steep slopes. Average elevation of the catchment is 1275-m above sea level. The highest elevation is at a mountain named Toprakdede Tepesi (1765 m) that is located in the eastern part of the catchment. A continental climate prevails in the basin, with very cold and rainy/snowy days in winter and very hot and dry weather in summer. Annual mean precipitation and mean
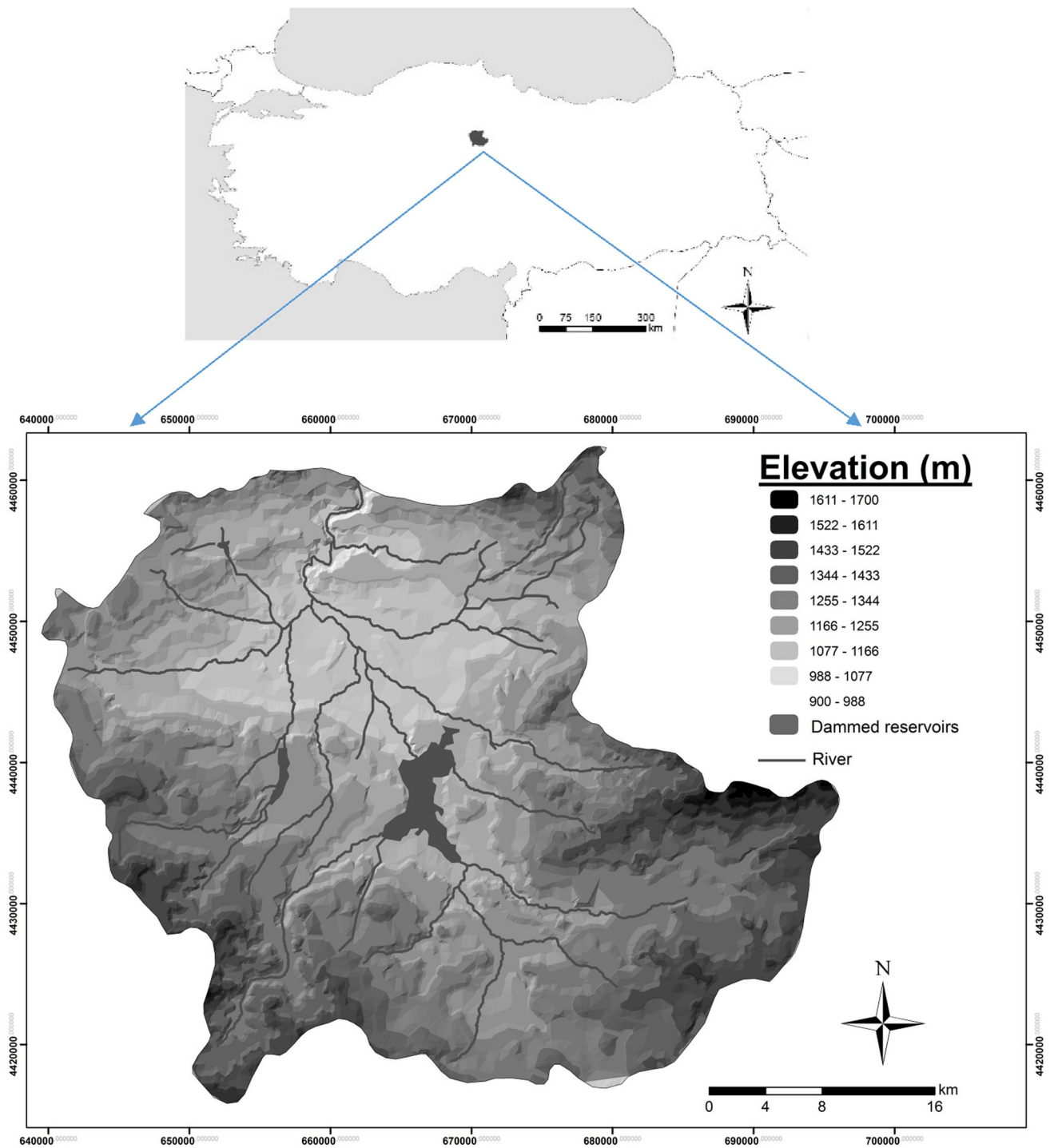
Fig. 1 Location map of the study area

temperature of the study area, which is different from the general Black Sea climate, are 364.8 mm and 9.5 °C, respectively. Koçhisar and Alaca reservoirs are two water storage structures in the catchment.

The soils of the basin are mainly brown soil (65.2 %) and brown forest soil (9.3 %). The distribution of the other

soil types in the study area is as follows: alluvial soil (6.9 %), chestnut soil (6.4 %), non-calcaric brown soil (6.3 %), and colluvial soil (5.9 %). In addition, 5 % of the area is composed of water surface, settlement areas, and bare rocks. The areas and ratios of the soil types were generated with GIS from 1:25,000 soil maps produced

14

Rend. Fis. Acc. Lincei (2017) 28:11–23

Table 1 Meteorological stations used in the study and computed MFI and R factor values for each station

Meteorology station	Coordinates (UTM-ED50, zone 36, m)		Altitude (m)	MFI	R factor mm ha^{-1} h^{-1} year^{-1}
	Easting	Northing			
Çorum–Boğazkale	636,869	4,431,331	1033	44.17	593.19
Yozgat–Merkez	655,406	4,409,834	1308	58.44	1111.07
Yozgat–Sorgun	686,672	4,408,011	1112	39.28	456.06
Tokat–Zile	745,680	4,464,620	728	42.89	555.4
Çorum–Mecitözü	694,639	4,488,477	782	39.63	465.27
Çorum–Merkez	663,954	4,490,173	778	41.00	502.02
Çorum–Sungurlu	619,323	4,447,844	783	41.83	525.03
Çorum–Ortaköy	691,515	4,460,403	799	39.01	449.03
Çorum–Alaca	656,644	4,447,304	931	35.59	365.64
Yozgat–Akdağmadeni	744,829	4,393,948	1335	53.54	913.11

MFI modified Fournier index, *R* rainfall erosivity factor

under the former United States of America classification system [United States Department of Agriculture (USDA) soil classification system 1938] and provided by the General Directorate of Rural Services of Turkey (KHGM). (Note: these soil maps have not yet been updated using the modern soil taxonomy classification system.)

2.2 Methods

2.2.1 The RUSLE model

The USLE model consists of a set of calculations to estimate soil erosion from a plot of land with homogeneous characteristics (Wischmeier and Smith 1978). The RUSLE model retains the general framework of the USLE but refines the calculations for each of the five erosion factors through greater temporal and spatial precision (Renard et al. 1997). With the RUSLE function, the average amount of soil loss is expressed as a function of five factors (Wischmeier and Smith 1965, 1978; Renard et al. 1997) as follows:

$$A = R \times K \times \text{LS} \times C \times P,$$

where A is the computed average amount of soil loss in Mg ha^{-1} year^{-1}, R is the rainfall-runoff erosivity factor (MJ mm ha^{-1} h^{-1} year^{-1}), K is the soil erodibility factor (Mg h MJ^{-1} mm^{-1}), LS is a combination of the slope length and steepness factors, C is the cover and management factor, and P is the support practices factor (LS, C, and P are dimensionless).

2.2.1.1 Rainfall erosivity factor (R) According to Wischmeier and Smith (1978), the rainfall erosivity (R) factor represents the effect of rainfall intensity on soil erosion and requires continuous, detailed data. To calculate the R factor

using monthly and annual rainfall data, Arnoldus (1980) reported a modified Fournier index (MFI):

$$\text{MFI} = \frac{\sum_{i=1}^{12}(pi)^2}{P},$$

where pi is the mean rainfall amount (mm) for month i, and P is the mean annual rainfall amount (mm).

According to Arnoldus (1980), the MFI is a good approximation of the R factor, with which it is linearly correlated. For the current investigation, precipitation data from 1960 to 2014 from ten meteorological stations located in and around the study area were collected, and the MFI was estimated for each station. Coordinate information of the meteorological stations is listed in Table 1.

To approximate the R factor using the calculated MFI for each station, the following R–MFI relationship, as suggested by Irvem et al. (2007) for a climatologically similar area, in terms of rainy days, amount and range of precipitation distributed over the four seasons, was used as follows:

$$R = 0.1215 \times \text{MFI}^{2.2421}.$$

The MFI and R values for each meteorological station were calculated, and the R factor map of the current study area was generated by interpolation in GIS.

2.2.1.2 Soil erodibility factor (K) K is defined as the rate of soil loss per unit of R as measured on a unit plot, and it accounts for the influence of soil properties on soil loss during storm events. The study area was divided into grid squares (Fig. 2).

A total of 348 soil samples were collected from the surface (0–20 cm) of the study area, according to the grid squares. The samples were transported to the laboratory where root material was removed, while the soil sample was being gently crumbled. These samples were used to
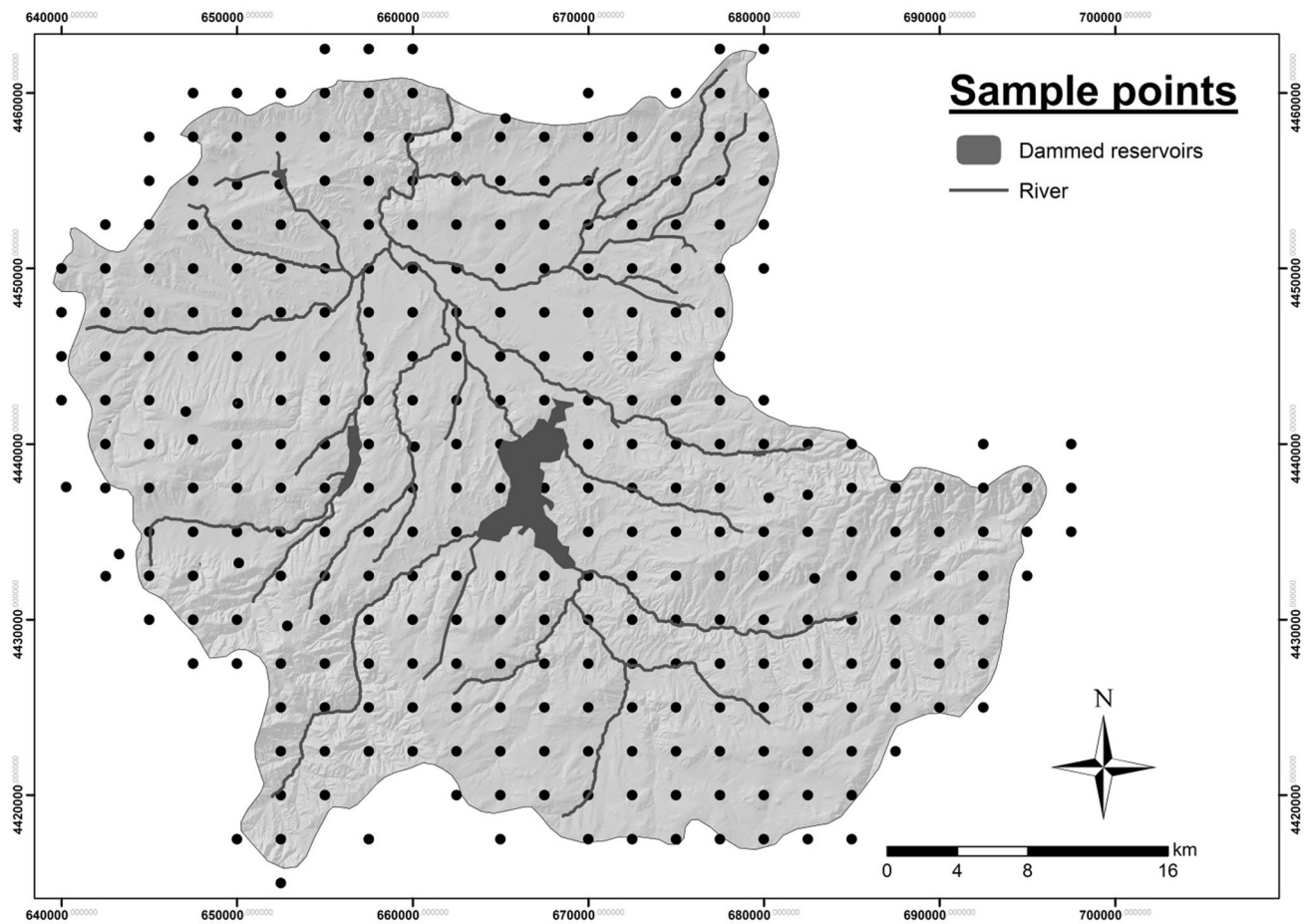
Fig. 2 Soil sampling design on the study area

determine physicochemical soil properties, including: sand %, silt %, clay %, organic matter %, structure, and permeability classes. The K values were computed from these soil properties with the following equation (Wischmeier and Smith 1978):

$$K = \frac{1}{100}\left\{2.1 \times 10^{-4} \times (12 - OM) \times [SI \times (SA + SI)]^{1.14} \right.$$
$$\left. + 2.5 \times (PE - 3) + 3.25 \times (ST - 2)\right\},$$

where K is expressed in units of Mg h MJ^{-1} mm^{-1}, and OM, SI, SA, PE, and ST are percentages of soil organic matter content, silt content, sand content, permeability class, and structure code, respectively. If soil organic matter content was equal to or greater than 4 %, OM was assumed constant at 4 % (Renard et al. 1997).

Soil samples were analyzed, and particle size distribution (Gee and Bauder 1986), hydraulic conductivity (Klute

Table 2 LULC classes and C factors

LULC class	C factor value
Broad-leaf forest	0.001
Coniferous forest	0.010
Sparsely coniferous forest	0.050
Heathland	0.038
Pasture	0.090
Vineyard and fruit orchards (agriculture)	0.180
Complex cultivation pattern (agriculture)	0.280
Rainfed agriculture	0.400
Irrigated agriculture	0.200
Water body	0.000
Pasture-rainfed agriculture	0.040
Forest-pasture	0.040
Bare rocks and construction sites	1.000

LULC land use and land cover, *C* land cover and management factor

16

Rend. Fis. Acc. Lincei (2017) 28:11–23

Table 3 Cross validation according to interpolation methods

Interpolation models	Power/semivariogram	RMSE		
		R	K	SOCD
IDW	1	247.3	0.0285	0.904
	2	254.1	0.0289	0.911
	3	265.0	0.0294	0.921
RBF	Completely regularized spline	254.3	0.0293	0.922
	Thin plate spline	307.4	0.0364	1.091
Kriging				
OK	Spherical	241.2	0.0285	0.902
	Exponential	241.0	0.0285	0.903
	Gaussian	241.2	0.0285	0.902
SK	Spherical	226.4	**0.0283**	**0.886**
	Exponential	**224.4**	0.0285	0.889
	Gaussian	227.4	0.0284	0.888
UK	Spherical	241.2	0.0285	0.902
	Exponential	241.0	0.0285	0.903
	Gaussian	241.2	0.0285	0.902

RMSE root mean square error, *IDW* inverse distance weighing, *RBF* radial basis function, *OK* ordinary kriging, *SK* simple, *UK* kriging universal kriging, *R* rainfall erosivity factor, *K* soil erodibility factor, *SOCD* soil organic carbon density
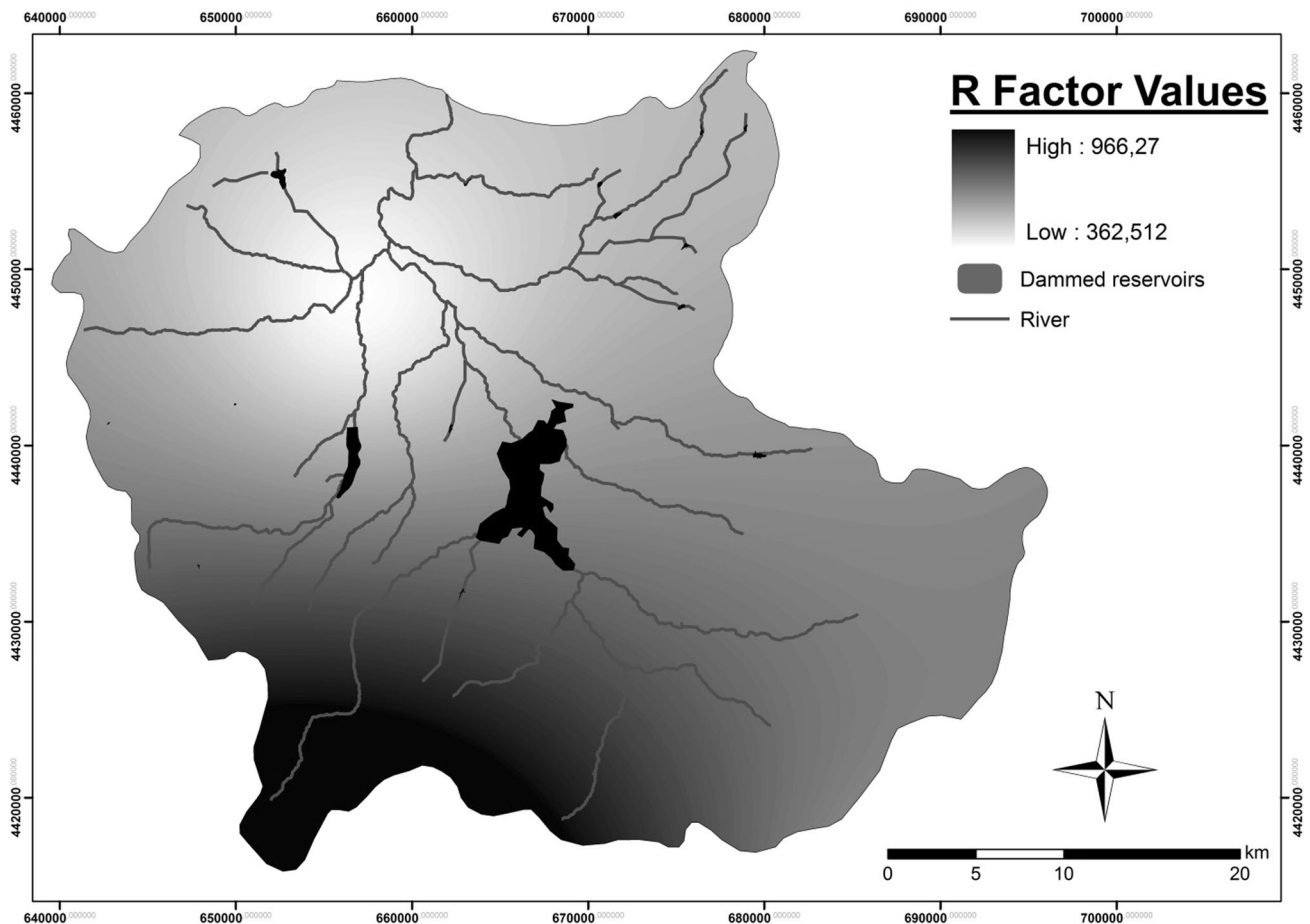
Fig. 3 The *R* factor map of the study area (MJ mm ha^{-1} h^{-1} year^{-1})

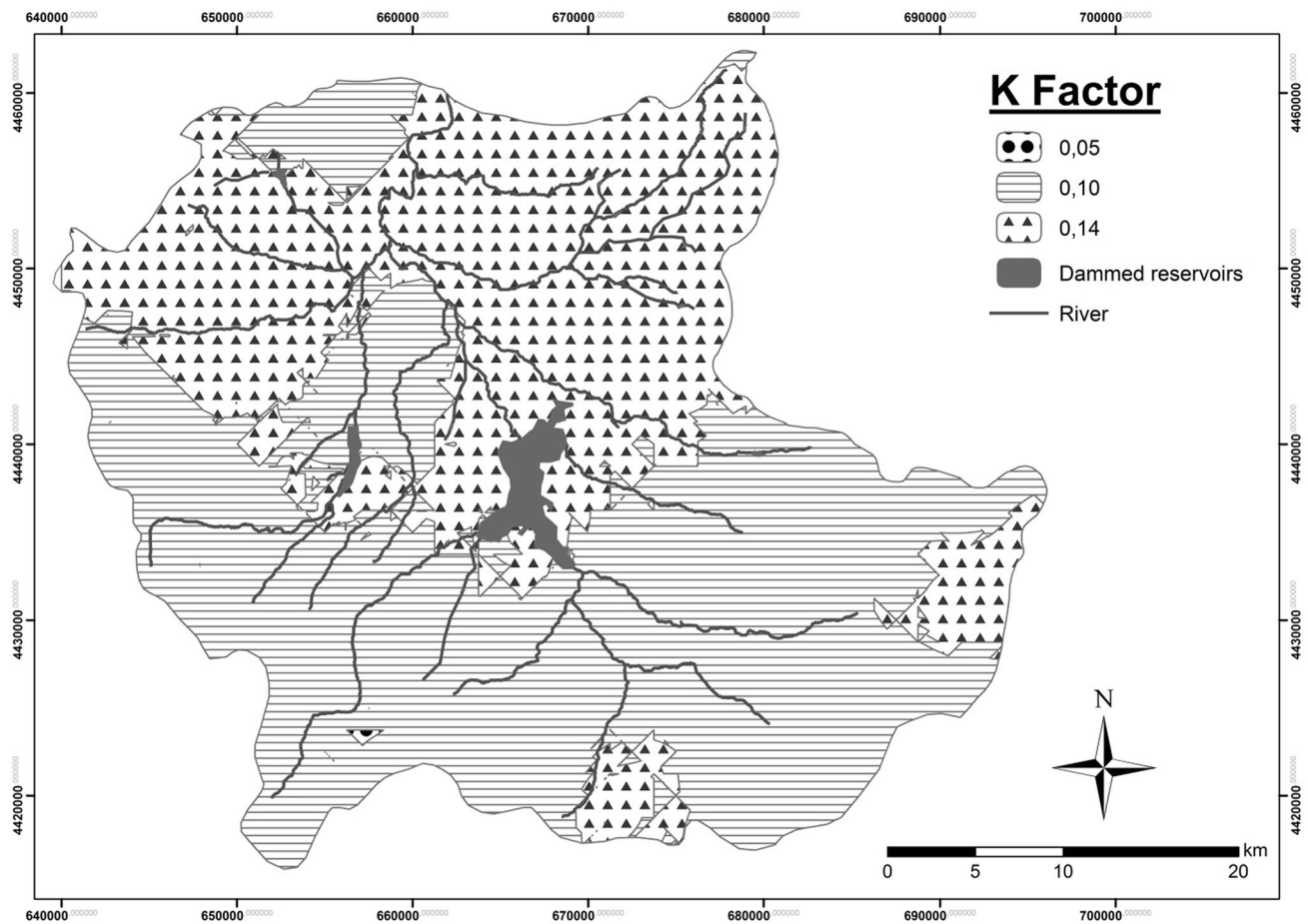**Fig. 4** The K factor map of the study area (Mg h MJ^{-1} mm^{-1})

and Dirksen 1986), aggregate stability (Kemper and Rosenau 1986), and organic matter content (Jackson 1958) were determined in the laboratory. The K factor map of the study area was generated with the interpolation models of GIS.

2.2.1.3 Slope length and steepness factor (LS) Slope is an important factor influencing overland flow generation and soil erosion, particularly beyond the critical slope degree. The slope length and steepness (LS) factor accounts for the effect of topography on soil erosion (Renard et al. 1997). Slope length is defined as the horizontal distance from the point of origin of the overland flow to the point where either the slope gradient decreases sufficiently for deposition to begin or runoff is concentrated in a defined channel (Wischmeier and Smith 1978). An increase in the LS factor indicates higher overland flow velocities and correspondingly greater erosion (Onori et al. 2006).

Hickey (2000), Boggs et al. (2001), Kinnel (2001), Gertner et al. (2002), Wang et al. (2003), and van Remortel et al. (2004) used digital elevation model (DEM) to estimate the LS factor. In the present study, the grid-based

DEM was generated from contour vector data which were digitized using a 1:25.000 scale topographic map.

2.2.1.4 Land cover and management factor (C) The land cover and management factor (C) is defined as the ratio of soil loss from land with specific vegetation cover to the corresponding soil loss from continuous fallow (Wischmeier and Smith 1978). In the present study, remotely sensed data were used to estimate the C distribution based on land use and land cover (LULC) classification results (Millward and Mersey 1999; Reusing et al. 2000), assuming that areas with the same amount of land cover have the same C values.

The supervised classification method (maximum likelihood) was used to produce the LULC classes, as described by Lillesand and Kiefer (2000), for determining the C factor. The LULC classes are listed in Table 2. The C factors used in this study were adopted from Renard et al. (1997), Yang et al. (2003) and İrvem and Tülücü (2004).

After creating the LULC map of the study basin, the C factors for the land classes were entered as attributes, and
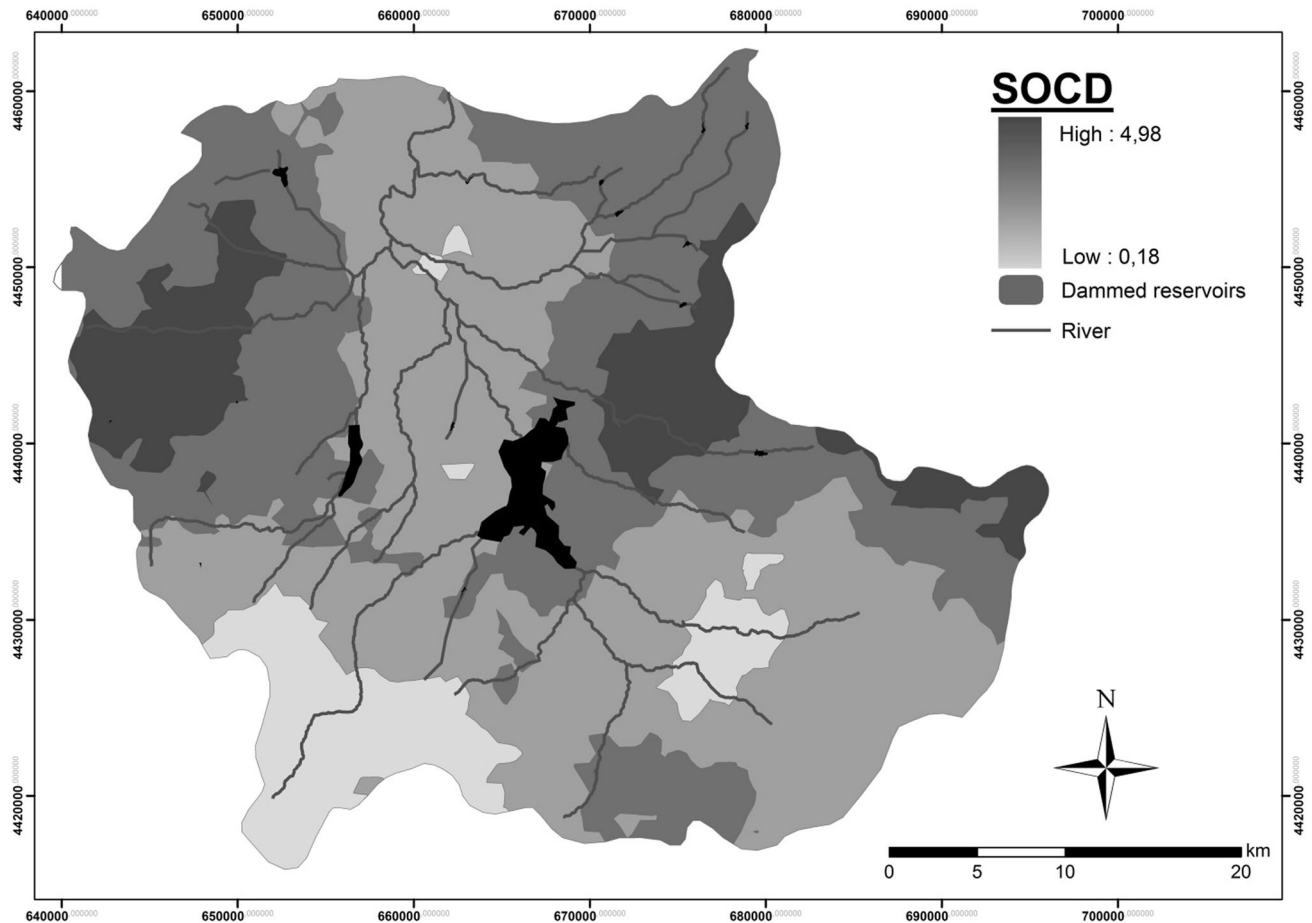
Fig. 5 Spatial distribution of SOCD (kg m^{-2})

a C factor map of the study area was generated using the reclassification method in the GIS.

2.2.1.5 Support practice factor (P)

Renard et al. (1997) indicated that the support practice factor (P) is the ratio of soil loss using a specific support practice to the corresponding loss with upslope and downslope tillage. As in most agricultural lands in Turkey, agricultural practices in the study area consist of upslope and downslope tillage without any conservation support practices, such as contouring or terracing. This situation is particularly evident during ground truthing observations. To remove the P factor from the soil erosion estimates, P was set at one, as suggested by Wischmeier and Smith (1978).

2.2.2 Soil organic carbon density estimation

Soil organic carbon density (SOCD) for each soil sample was estimated with the following equation:

$$SOCD_D = \frac{(1 - \delta_i\,\%) \times \rho_i \times C_i \times T_i}{100},$$

where $SOCD_D$ represents the SOC density of a soil sample with a depth (20 cm); $\delta_i\,\%$ represents the volumetric percentage of the fraction >2 mm (rock fragments), ρ_i is the bulk density (g cm^{-3}), C_i is the SOC content (g kg^{-1}), and T_i represents the thickness (cm) of the layer i.

2.2.3 Interpolation analysis

In this study, different interpolation methods (inverse distance weighing—IDW, radial basis function—RBF and kriging) were applied for predicting the spatial distribution of R, K and SOCD. Kriging is a geostatistical technique similar to IDW in that it uses a linear combination of weights at known points to estimate the value at an unknown point. Kriging uses a semivariogram, a measure of spatial correlation between two points, so that weightings change according to the spatial arrangement of the samples. In contrast to other estimation procedures, kriging provides a measure of the error or uncertainty of the estimated surface. Several forms of kriging interpolation exist, including ordinary kriging (OK), simple kriging (SK), and universal kriging (UK).
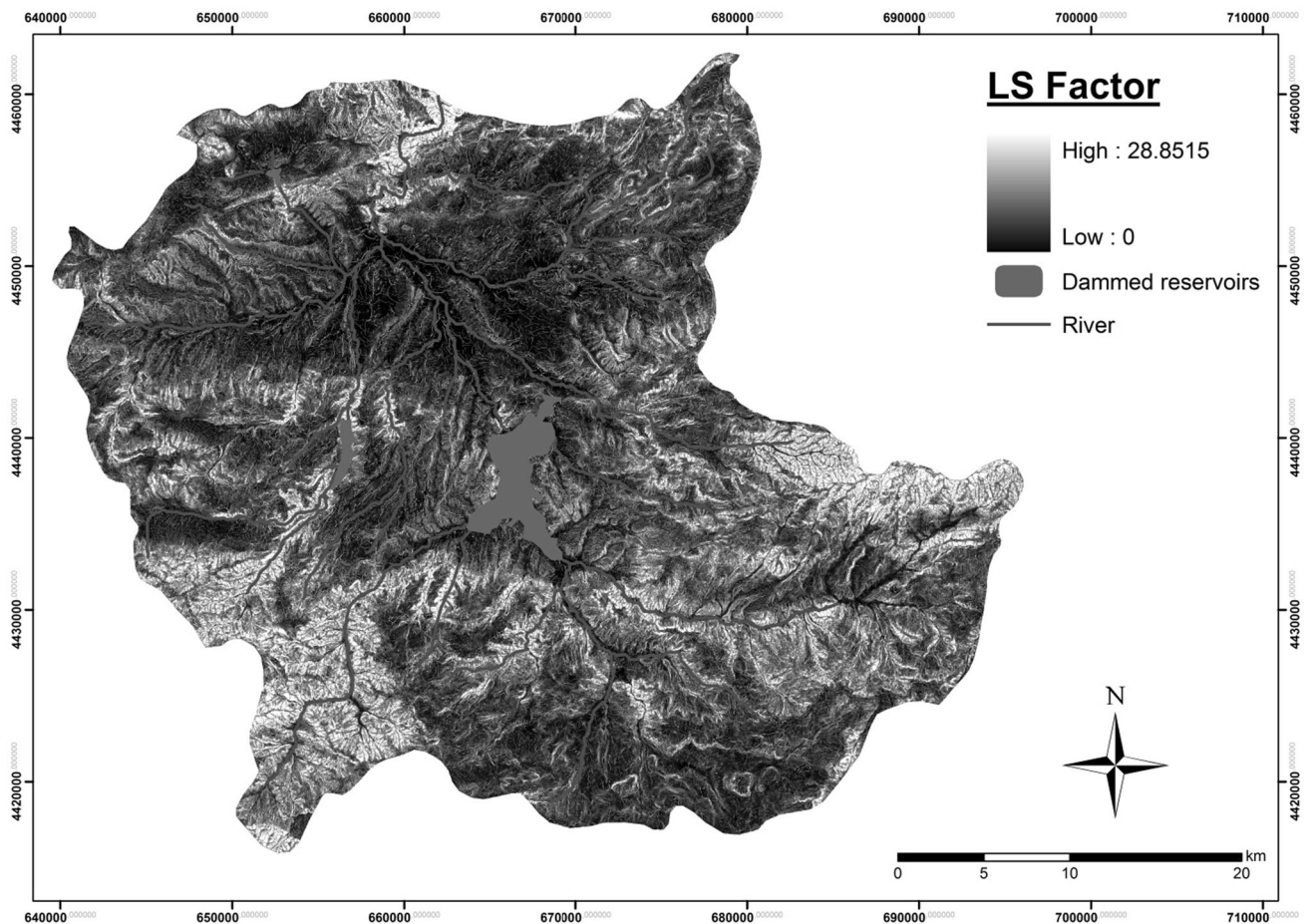
Fig. 6 The LS factor map of the study area

In the present study, root mean square error (RMSE) was used to evaluate the interpolation techniques, with the lowest RMSE indicating the most accurate prediction. Estimates were determined with the following formula:

$$\text{RMSE} = \sqrt{\frac{\sum (z_{i*} - z_i)^2}{n}},$$

where z_i is the predicted value, z_{i*} is the observed value, and n is the number of observations.

3 Results and discussion

3.1 Distribution of R, K, and SOCD was determined with geostatistical analysis

Interpolation analyses for R, K, and SOCD were used to identify the best predictive model from among 14 different semivariogram models, namely, inverse distance weighting—IDW with weightings of 1, 2, and 3 powers and radial basis function—RBF with thin plate spline (TPS), ordinary kriging (OK), simple kriging (SK), and universal kriging (UK) with spherical, exponential, and Gaussian variograms. Following that, the variogram or function of each interpolation method yielding the best results was determined. Comparison of interpolation methods for R, K, and SOCD is provided in Table 3. Finally, according to the interpolation analyses, simple kriging with the spherical model was used to estimate or predict K and SOCD, while the exponential model was found to determine the R value at unsampled locations. The spatial distribution maps of R, K, and SOCD are shown in Figs. 3, 4 and 5.

Figure 4 shows the R factor map of the study area. The average annual R factor ranged from 362.51 to 966.27 MJ mm ha^{-1} h^{-1} year^{-1}. The computed MFI and R factors for each meteorological station are listed in Table 1. There was more rainfall erosivity in the southwestern part than in the north and north-eastern parts, because rainfall erosivity is closely related to precipitation, which increases from north to south in the catchment (Fig. 3).

Başkan and Dengiz (2008) compared soil erodibility (K) maps prepared by traditional and geostatistical methods
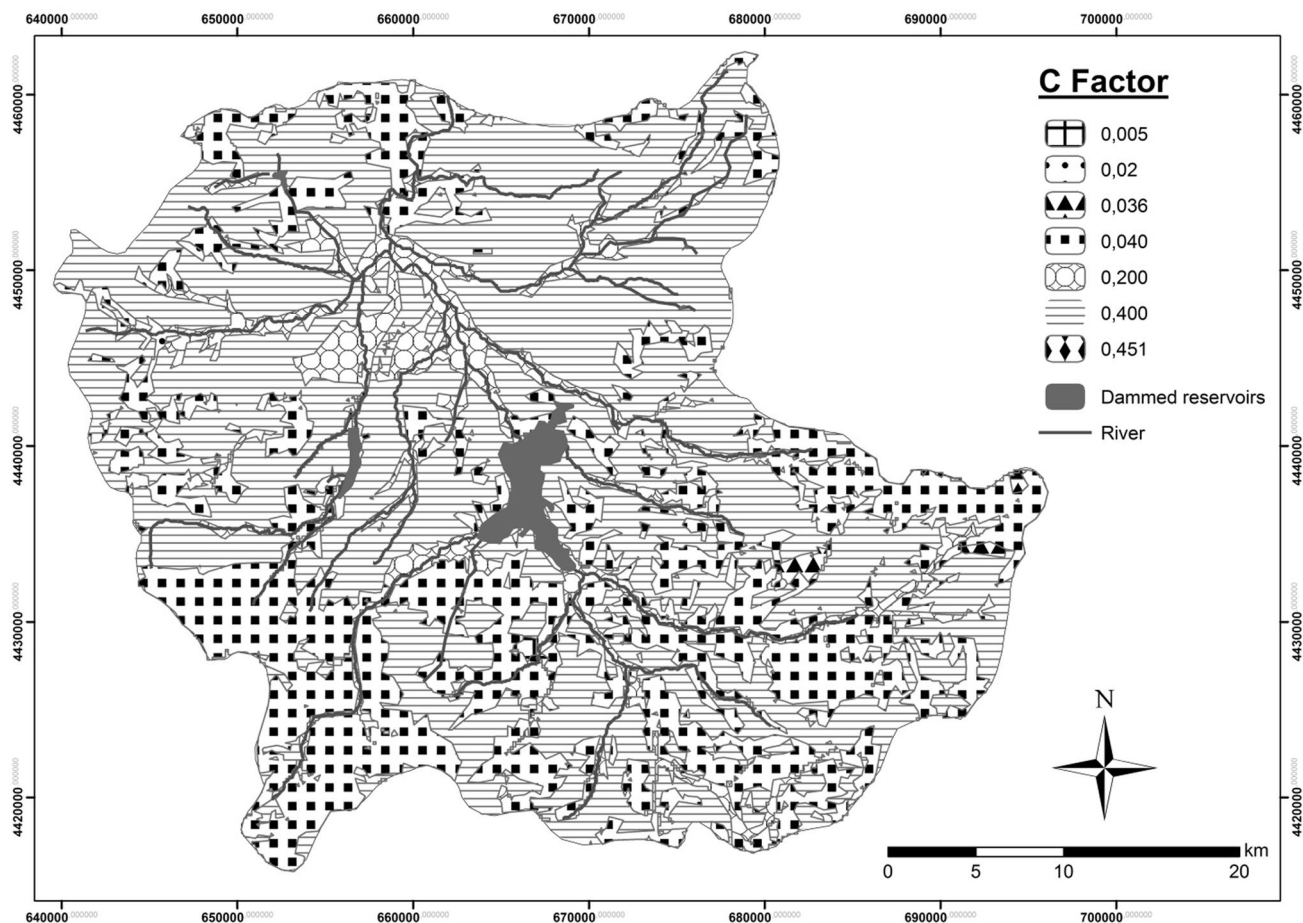
20

Rend. Fis. Acc. Lincei (2017) 28:11–23

Fig. 7 The C factor map of the study area

for Sogulca Basin soils and reported that a kriged K map displayed significantly better results than a K map developed with traditional methods. Figure 4 shows the map for the K factor, generated with the geostatistical approach, which varied from 0.01 to 0.14 Mg h MJ^{-1} mm^{-1}. The K factors were low in the southwest and southeast of the study area, whereas high K values were determined in northern parts of the catchment where the river has formed and streamed throughout an alluvial land located almost in the central part of the catchment at the discharge point into Koçhisar Dam. The K values were also typically high in the eastern parts of the catchment on steep slopes where mostly medium and sandy textured soils occur.

In this study, for the SOCD in surface soil (0–20 cm), the isotropic spherical model provided the best fit for the computed semi-variance points (the distribution map of SOCD of the surface soil is shown in Fig. 5). In addition, SOCD values were between 0.18 and 4.92 kg m^{-2} in the catchment (Fig. 5). Guggenberger et al. (1995) stated that the type of land use system is an important determinant of SOC levels, particularly in top soils. Furthermore, changes

in land use and management practices influence the amount and rate of SOCD gain or loss.

3.2 Slope length and steepness (LS)

Figure 6 shows the map of the LS distribution, which ranged from 0.01 in the flat areas in the north-central part of the basin to 28.85 in the highlands (elevation approximately 1700 m) in the Southwestern, and some northern parts of the basin which have the steepest slopes, the greatest variability in elevation and high LS values. The LS values were highest in the mountainous areas and deep valleys. These areas were mostly located in the upper part of the basin.

Figure 7 shows the map of the C generated from satellite imagery and forest inventory for the LULC map of the study area. The study area was composed of 57.6 % rainfed agricultural lands, 32.2 % mixed rain-fed agriculture and pasture, 9.2 % irrigated agriculture 0.9 % sparse coniferous forest and pasture, and 0.1 % bare rocks, artificial area, and water bodies. The C values ranged from 0 to 1.0 (Table 2) and were especially low in southwestern parts
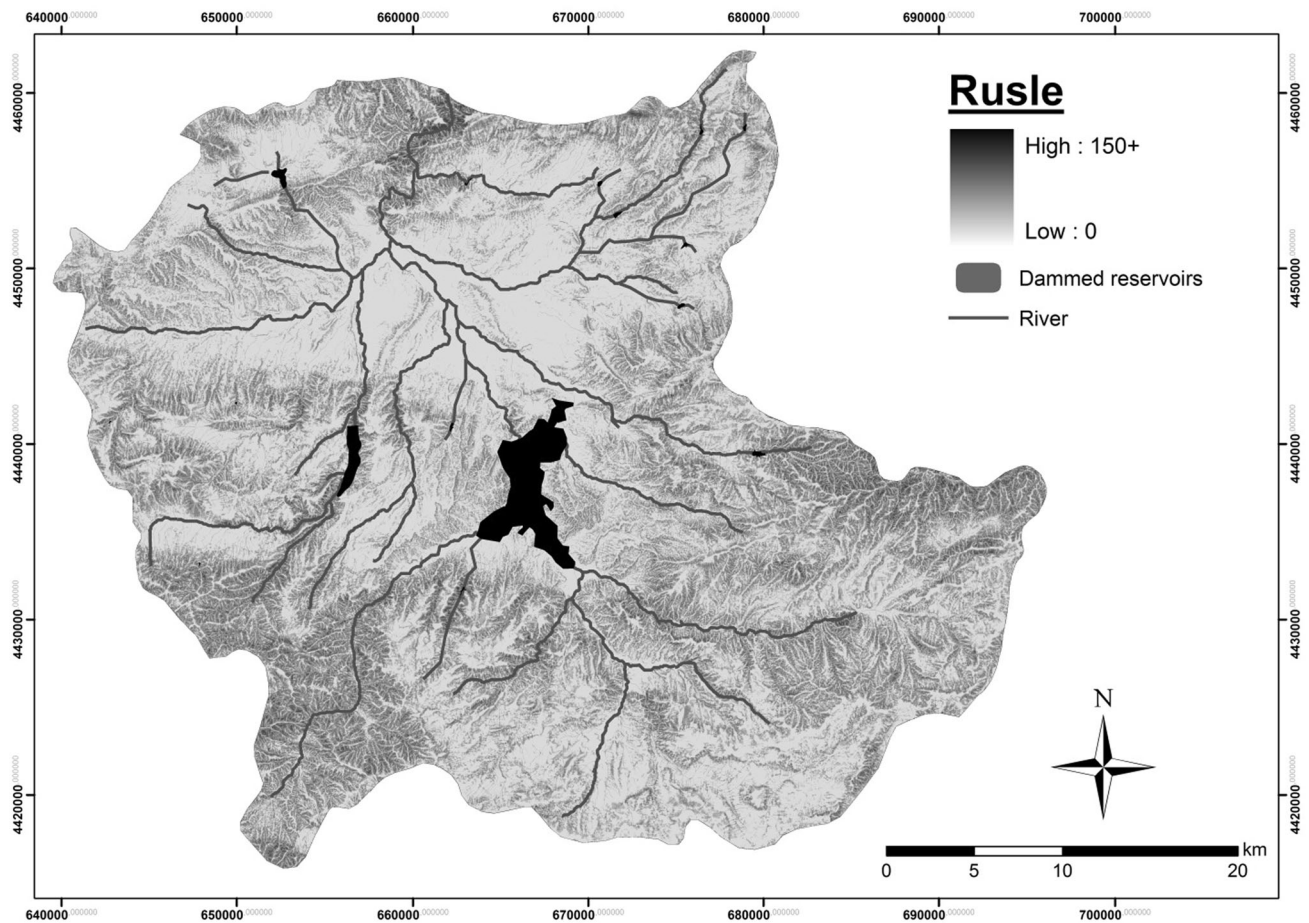
Fig. 8 Distribution the different soil erosion classes for the study area

of the basin, indicating that forests (broad leaf and coniferous forests) and some pasture land have low erosion risk, but most of the cultivated and fallow agricultural land and degraded pasture areas have high or very high erosion potential.

The *P* factor should be increased in agricultural areas to decrease soil erosion to an acceptable level. However, in flat or almost flat areas, where agriculture is the main land use type, the erosion risk was found to be low (note: no supporting practice was observed in the study area). Therefore, the *P* value of 1 was not used in calculations (Wischmeier and Smith 1978; Çanga 1985).

The RUSLE function estimates only local erosion amounts and cannot be used to estimate the sediment yield for an entire watershed (Renard et al. 1997). The map of the potential soil losses predicted by the RUSLE as a product of *R*, *K*, LS, and *C* is shown in Fig. 8. Annual soil losses in tonnes per hectare per year with respect to the different soil erosion classes of Bergsma et al. (1996) are provided in Table 4. Table 4 shows that more than the half of the study area is in the very low and low erosion risk classes which range from 0 and 12 t ha^{-1} year^{-1}, whereas

Table 4 Annual soil loss predicted for the different soil erosion classes of the study area

Description	Classes (t ha^{-1} year^{-1})	Area (km^2)	Ratio (%)
Very low	0–5	852.85	51.5
Low	5–12	391.32	23.6
Moderate	12–35	339.87	20.5
High	35–60	54.78	3.3
Very high	60–150	16.18	1.0
Severely	150+	1.4	0.1
Total		1656.4	100

4.4 % of the total area (723.6 ha) is under high and very high erosion risk of 35 to 150 t ha^{-1} year^{-1}.

4 Conclusions

The RUSLE model was applied to estimate soil loss with RS and GIS in the Alaca catchment located in the Central Black Sea region of Turkey. Detailed

pluviograph data for calculating the *R* factor were not available. Therefore, the R factor was estimated with MFI data based on mean annual and monthly rainfall data from the meteorological stations located in and around the study area. Existing soil data were inadequate for the determination of the *K* factor. A new *K* map was produced by collecting soil samples from the field and using a geostatistical method. An SODC map was also produced. The LS values were estimated with a GIS program automated hydrologic procedure to calculate the slope length and steepness using DEM. The *C* values were determined from the LULC map of the study area, which was derived from satellite images and from forest inventories. The *P* factor was assumed to be 1, meaning that soil conservation support practices were not used in the study area, as confirmed by field observations. Soils and topographical properties of the watershed had a greater influence on the magnitude of potential soil losses than land use/land-cover type, since the R factor did not change significantly in the study area. In addition, the distribution of SOC losses almost matched the distribution of soil erosion risk classes in the study area. Particularly, carbon levels on south west and northwest parts of the study area associated with high soil erosion levels.

The RUSLE erosion model is very useful for the assessment of erosion risk status, because the conventional methods impose high time and labor costs for data collection, including the measurement of soil erosion in heterogeneous, patchy, and large areas. Bayramin et al. (2003) stated that these problems can be overcome using predictive models and new techniques. With GIS, the collected data can be easily analyzed and used to map soil erosion risk and prepare a land management plan for the sustainable use of land resources. Moreover, the model can identify the areas with erosion risk for decision-makers, so that they can develop soil and water conservation plans in general, including research in the areas of high erosion risk to mitigate the problem.

Finally, the application of the RUSLE methodology produced a consistent pattern of soil erosion mapping among different land uses, slope positions, and soil groups and reasonably predicted the potential annual soil losses, including the identification of the most erosion-prone areas due to concentrated flow. This approach can also be used to determine the area's most sensitive to soil erosion on a regional scale, which could help facilitate comprehensive soil conservation management and sustainable land use practices.

References

Arnoldus HMJ (1980) An approximation of the rainfall factor in the universal soil loss equation. In: De Boodt M, Gabriels D (eds) Assessment of erosion. Wiley, Chichester, pp 127–132

Başkan O, Dengiz O (2008) Comparision of traditional and geostatistical methods to estimate soil erodibility factor. Arid Land Res Manag 22:29–45

Bayramin İ (1998) İntegrating digital terrain and satellite image data with soils data for small scale mapping of soils. PhD thesis, Purdue University Agronomy Department, p 121

Bayramin İ, Dengiz O, Baskan O, Parlak M (2003) Soil erosion risk assessment with ICONA model, case study: Beypazari area. Turk J Agric For 27:105–116

Bergsma E, Charman P, Gibbons F, Hurni H, Moldenhauer WC, Panichapong S (1996) Terminology for soil erosion and conservation. International Society of Soil Science, Grafisch Service Centrum, Wageningen

Boggs G, Devonport K, Evans K, Puig P (2001) GIS-based rapid assessment of erosion risk in a small catchment in the wet/dry tropics of Australia. Land Degrad Dev 12:417–434

Burrough PA (1986) Principles of geographical information system for land resources assessment. Oxford University Press, Oxford

Çanga MR (1985) Toprak ve su koruma. Atatürk Üniversitesi Ziraat Fakültesi Yayınları No 1386 Ders Kitabı No 400 (**in Turkish**)

Csafordi P, Pödör A, Bugc J, Gribovszki Z (2012) Soil erosion analysis in a small forested catchment supported by ArcGIS model builder. Acta Silv Lign Hung 8:39–55

Dengiz O, Saglam M, Türkmen F (2015) Effects of soil types and land use-land cover on soil organic carbon density at Madendere Watershed. Eurasian J Soil Sci 4:82–87

Edwards JA, Koval EJ, Lendt BW, Ginther PG (2008) Distribution system model development and maintenance using GIS, guidelines and recommended procedure. Black and Veatch internal whitepaper, Kansas City

Eedy W (1995) The use of GIS in environmental assessment. Impact Assess 13:199–206

Gee GW, Bauder JW (1986) Particle-size analysis. In: Klute A (ed) Methods of soil analysis part 1 physical and mineralogical methods, vol 9, part 1, 2nd edn. American Society of Agronomy, Madison, WI, pp 383–441

Gertner G, Wang G, Fang S, Anderson AB (2002) Effect and uncertainty of digital elevation model spatial resolutions on predicting the topographical factor for soil loss estimation. J Soil Water Conserv 57(3):164–182

Guggenberger G, Zech W, Thomas RJ (1995) Lignin and carbohydrate alteration in particle size separates of an Oxisol under tropical pastures following native savanna. Soil Biol Biochem 27:1629–1638

Hickey R (2000) Slope angle and slope length solutions for GIS. Cartography 29(1):1–8

İrvem A, Tülücü K (2004) Coğrafi bilgi sistemi ile toprak kaybı ve sediment verimi tahmin modelinin (est) oluşturulması ve Seyhan-Körkün alt havzasına uygulanması. Çukurova Üniversitesi Fen Bilimleri Enstitüsü Dergisi 13 (**in Turkish**)

İrvem A, Topaloglu F, Uygur V (2007) Estimating spatial distribution of soil loss over Seyhan River Basin in Turkey. J Hydrol 336:30–37

Jackson ML (1958) Soil chemical analysis. Prentice Hall Inc., Englewood Cliffs

Jones RJA, Montanarella L (2003) Land degradation. The JRC Enlargement Action, Contributions to the International Workshop Soil and Waste Unit Institute for Environment & Sustainability Joint Research Centre European Commission Ispra 21020 Italy, p 333

Kemper WD, Rosenau RC (1986) Aggregate stability and size distribution. In: Klute A (ed) Methods of soil analysis part 1 physical and mineralogical methods, vol 9, 2nd edn. Agronomy, Madison, pp 425–442

Kinnel PIA (2001) Slope length factor for applying the USLE-M to erosion in grid cells. Soil Tillage Res 58:11–17

Klute A, Dirksen C (1986) Hydraulic conductivity and diffusivity. In: Klute A (ed) Methods of soil analysis part 2 agronomy, vol 9. Am Soc Agron Inc, Madison, pp 687–732

Lillesand TM, Kiefer RW (2000) Remote sensing and image interpretation, 4th edn. Wiley, New York

Lu D, Li G, Valladares GS, Batistella M (2004) Mapping soil erosion risk in Rondonia, Brazilian Amazonia: using RUSLE, remote sensing and GIS. Land Degrad Dev 15:499–512

Martin A, Gunter J, Regens J (2003) Estimating erosion in a riverine watershed, Bayou Liberty-Tchefuncta River in Louisiana. Environ Sci Pollut Res 4:245–250

Meyer LD (1980) Soil conservation problems and prospects. In: Morgan RCP (ed) International Conference on Soil Conservation the Natural College of Agricultural Engineering, Silsoe Bedford, UK

Millward AA, Mersey JE (1999) Adapting the RUSLE to model soil erosion potential in a Mountainous Tropical Watershed. Catena 38:109–129

Ministry of Agriculture, Forestry and Villages (1987) General management planning of turkey (soil conservation main plan). Ministry of Agriculture Forestry and Villages, General Directorate of Rural Services, Ankara, p 105

Onori F, De Bonis P, Grauso S (2006) Soil erosion prediction at the basin scale using the revised universal soil loss equation (RUSLE) in a catchment of Sicily (southern Italy). Environ Geol 50:1129–1140

Ouyang D, Bartholic J (2001) Web-based GIS application for soil erosion prediction. In: Proceedings of an International Symposium—Soil Erosion Research for the 21st Century, Honolulu, HI, 3–5 Jan 2001, pp 260–263

Pla I (2008) Desertification under climate change and changing land use in Mediterranean environments. In: Gabriels D, Cornelis W, Eyletters M, Hollebosh P (eds) Combating desertification assessment adaptation and mitigation strategies. UNECO Chair of Eremology Ghent University, Belgium, pp 30–40

Renard KG, Foster GR, Weeies GA, Porter JP (1991) RUSLE: revised universal soil loss equation. J Soil Water Conserv 46:30–33

Renard K, Foster G, Weesies G, McCool D, Yoder D (1997) Predicting soil erosion by water: a guide to conservation planning with the revised universal soil loss equation (RUSLE). USDA Agr Handbook No 703. United States Department of Agriculture, Agriculture research Service, Washington, DC

Reusing M, Schneider T, Ammer U (2000) Modeling soil erosion rates in the Ethiopian Highlands by integration of high resolution MOMS-02/D2-stereo-data in a GIS. Int J Remote Sens 21:1885–1896

RIVM (2000) Technical report on soil degradation. RIVM report 481505018, Bilthoven

UNCCD (2015) United Nations convention to combat desertification. Living Land 192, UNCCD and Copublisher. ISBN: 978-92-95043-24-4. http://www.unccd.int/en/resources/publication/Pages/default.aspx

Van Remortel RD, Maichle RW, Hickey RJ (2004) Computing the LS factor for the revised universal soil loss equation through array based slope processing of digital elevation data using C^{++} executable. Comput Geosci 30:1043–1053

Wang G, Gertner G, Fang S, Anderson AB (2003) Mapping multiple variables for predicting soil loss by geostatistical methods with TM images and a slope map. Photogramm Eng Remote Sens 69:889–898

Wischmeier WH, Smith DD (1965) Predicting rainfall erosion losses from cropland east of the Rocky Mountains: guide for selection of practices for soil and water conservation planning. USDA agriculture handbook. US Government Printing Office, Washington

Wischmeier WH, Smith DD (1978) Predicting rainfall erosion losses—a guide to conservation. Agricultural handbook 537. Planning Science and Education Administration US Dept. of Agriculture, Washington, p 58

Yang D, Kanae S, Oki T, Koikel T, Musiake T (2003) Global potential soil erosion with reference to land use and climate change. Hydrol Process 17(14):2913–2928